Manadoperoxides A−D from the Indonesian Sponge *Plakortis* cfr. *simplex*. Further Insights on the Structure−Activity Relationships of Simple 1,2-Dioxane Antimalarials

Caterina Fattorusso,[†] Marco Persico,[†] Barbara Calcinai,[‡] Carlo Cerrano,[§] Silvia Parapini,[⊥] Donatella Taramelli,[⊥] Ettore Novellino,[∥] Adriana Romano,[†] Fernando Scala,[†] Ernesto Fattorusso,[†] and Orazio Taglialatela-Scafati*[,†]

Dipartimento di Chimica delle Sostanze Naturali, Università di Napoli "Federico II", Via D. Montesano, 49, I-80131, Napoli, Italy, Dipartimento di Scienze del Mare, Università Politecnica delle Marche, Via Brecce Bianche, 60131 Ancona, Italy, Dipartimento per lo Studio del Territorio e delle sue Risorse, Università di Genova, Corso Europa 26, 16132, Genova, Italy, Dipartimento di Sanità Pubblica-Microbiologia-Virologia, Università degli Studi di Milano, Via Pascal, 36, Milano, Italy, and Dipartimento di Chimica Farmaceutica e Tossicologica, Università di Napoli "Federico II", Via D. Montesano, 49, I-80131, Napoli, Italy

Received March 31, 2010

The new endoperoxyketal polyketides manadoperoxides A−D (**2**−**5**) have been isolated from the Indonesian sponge *Plakortis* cfr. *simplex* and their stereostructures established by means of spectroscopic data and semisynthetic transformations. Manadoperoxides were assayed *in vitro* against D10 and W2 strains of *Plasmodium falciparum* and showed moderate antimalarial activity compared to that of plakortin (**1**) and peroxyplakoric B_3 ester (**9**), the latter differing from manadoperoxide B only by minor structural details. This unexpected difference in the antimalarial activity has been rationalized on the basis of our recently published model for the interaction of 1,2-dioxanes with heme and production of C-centered radicals toxic to the parasite. For the manadoperoxides, either the endoperoxide linkage is inaccessible to the heme iron or the O1 radical cannot evolve to produce a C-centered radical.

Malaria, an infection caused by different species of *Plasmodium* protozoa, involves over 400 million clinical cases and at least one million deaths each year. A rise in mortality has been experienced in recent years, principally due to the multidrug resistance of parasites to the available antimalarials.[1]

The development of endoperoxide-based drugs can be considered one of the most remarkable advancements in malaria chemotherapy over the last few decades. Research in this field began in 1976 with the isolation and identification of artemisinin, an endoperoxide sesquiterpene lactone possessing a 1,2,4-trioxane moiety, from *Artemisia annua* leaves.[2] Artemisinin and, principally, its derivatives possess potent activity against chloroquine-resistant strains of *Plasmodium falciparum*, and they are currently fundamental for antimalarial combination therapy (ACT). However, their therapeutic value is limited by the modest oral availability, the short half-life, and the risk of embryotoxicity.[3] In addition, given the unsuitability of total synthesis, all of the production of artemisinin relies on the extraction from the natural source, which is costly and low-yielding.[4] The recent reports of clinical resistance to artesunate in Southeast Asia further draw attention to the necessity of rapidly finding reliable alternatives to artemisinin.[5]

The marine environment and, in particular, invertebrate organisms such as Porifera appear as an attractive source of chemodiversity to exploit in the design of new antimalarial compounds. In a recent review we have listed a number of endoperoxide derivatives, isolated from marine invertebrates, showing promising antimalarial activity *in vitro*.[6] Among them, plakortin (**1**), an endoperoxide polyketide obtained from the Caribbean sponge *Plakortis simplex,* was particularly attractive, as it showed activity in the nanomolar range against chloroquine-resistant strains of *P. falciparum in vitro*.[7,8] Evaluation of the antimalarial activity of natural analogues[9] and semisynthetic derivatives,[10] interpreted in the light of computational calculations,[10,11] allowed us to postulate a detailed mechanism for the antimalarial action of simple 1,2-dioxanes,[11] which may possibly pave the way for the rational design of new endoperoxides with optimized antimalarial activity.

In our ongoing screening for bioactive secondary metabolites from Indonesian marine invertebrates,[12,13] we recently had the opportunity to analyze a specimen of *P.* cfr. *simplex* collected in the Bunaken Marine Park of Manado (North Sulawesi, Indonesia). From the organic extract of this sponge we have obtained four new peroxyketal polyketides, which we named manadoperoxides A−D (**2**−**5**), and herein we describe their isolation, stereostructural characterization, and antimalarial activity. The isolation of the manadoperoxides represented a convenient opportunity to extend the structure−activity relationships previously established for the antimalarial activity of the plakortin family.

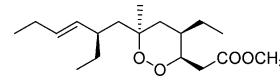

1

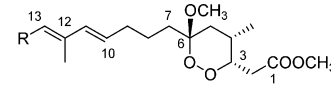

2 R = CH_3
3 R = CH_2CH_3

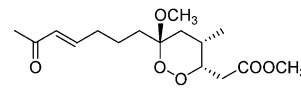

4

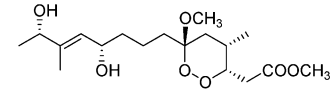

5

Results and Discussion

The sponge *P.* cfr. *simplex* (order Homosclerophorida, family Plakinidae) was collected in January 2008 along the coast of Bunaken Island. After homogenization, the organism was exhaustively extracted sequentially with MeOH and $CHCl_3$. The combined extracts were subjected to chromatography over silica followed by repeated column and HPLC chromatographies (*n*-hexane/EtOAc mixtures) to afford manadoperoxides A−D (**2**−**5**) in the pure state.

Manadoperoxide A (**2**) showed pseudomolecular ion peaks at *m/z* 327 $[M + H]^+$ and 349 $[M + Na]^+$ in the positive ESI mass spectrum, while HR measurements assigned the molecular formula $C_{18}H_{30}O_5$ to **2**, implying four unsaturation degrees. Analysis of ^1H

* To whom correspondence should be addressed. Tel: +39-081-678509. Fax: +39-081-678552. E-mail: scatagli@unina.it.
[†] Dipartimento di Chimica delle Sostanze Naturali, Università di Napoli "Federico II".
[‡] Università Politecnica delle Marche.
[§] Università di Genova.
[⊥] Università degli Studi di Milano.
[∥] Dipartimento di Chimica Farmaceutica e Tossicologica, Università di Napoli "Federico II".

10.1021/np100196b
Published on Web 06/03/2010

Table 1. ^{1}H (500 MHz) NMR Data of Manadoperoxides A (**2**), C (**4**), and D (**5**) in $CDCl_3$

pos.	**2** δ_H, mult. (*J* in Hz)	**4** δ_H, mult. (*J* in Hz)	**5** δ_H, mult. (*J* in Hz)
2a	2.97, dd (15.5, 9.5)	2.93, dd (15.7, 9.6)	2.94, dd (15.5, 9.5)
2b	2.44, dd (15.5, 4.5)	2.46, dd (15.7, 4.1)	2.46, dd (15.5, 4.3)
3	4.43, ddd (9.5, 4.5, 3.0)	4.46, ddd (9.6, 4.1, 3.0)	4.44, ddd (9.5, 4.3, 3.0)
4	2.57, m	2.56, m	2.58, m
5a	1.68[a]	1.73[a]	1.68[a]
5b	1.28[a]	1.29[a]	1.33
7a	1.66[a]	1.69[a]	1.63[a]
7b	1.32[a]	1.30[a]	1.34[a]
8a	1.40[a]	1.53, m	1.42[a]
8b	1.40[a]	1.53, m	1.35[a]
9a	2.07, m	2.25[a]	1.64[a]
9b	2.07, m	2.25[a]	1.55, m
10	5.47, dt (15.9, 6.0)	6.78, dt (16.4, 6.6)	4.40, m
11	6.03, d (15.9)	6.18, d (16.4)	5.45, d (8.7)
13	5.44, bq (6.9)		4.22, q (7.1)
14	1.69[a]		1.27, d (7.1)
4-Me	0.84, d (7.1)	0.85, d (7.1)	0.86, d (7.1)
12-Me	1.70, bs	2.25, s	1.71, bs
1-OMe	3.72, s	3.72, s	3.73, s
6-OMe	3.25, s	3.27, s	3.27, s

[a] Overlapped with other signals.

Table 2. ^{13}C (125 MHz) NMR Data of Manadoperoxides A (**2**), C (**4**), and D (**5**) in $CDCl_3$

pos.	**2** δ_C, mult.	**4** δ_C, mult.	**5** δ_C, mult.
1	171.9, C	172.3, C	172.2, C
2	31.8, CH_2	31.4, CH_2	31.7, CH_2
3	80.1, CH	79.8, CH	79.7, CH
4	27.6, CH	27.1, CH	27.2, CH
5	34.6, CH_2	34.4, CH_2	34.5, CH_2
6	103.4, C	103.0, C	103.0, C
7	32.4, CH_2	34.3, CH_2	31.4, CH_2
8	23.6, CH_2	21.8, CH_2	22.0, CH_2
9	33.7, CH_2	32.6, CH_2	38.4, CH_2
10	126.0, CH	147.0, CH	70.1, CH
11	135.8, CH	132.1, CH	127.1, CH
12	133.3, C	198.7, C	142.0, C
13	124.8, CH		72.8, CH
14	12.2, CH_3		17.9, CH_3
4-Me	17.0, CH_3	17.2, CH_3	17.1, CH_3
12-Me	13.0, CH_3	27.3, CH_3	13.7, CH_3
1-OMe	52.2, CH_3	52.2, CH_3	52.2, CH_3
6-OMe	48.8, CH_3	48.8, CH_3	48.7, CH_3

and ^{13}C NMR spectra of **2** ($CDCl_3$, Tables 1 and 2), guided by inspection of the 2D HSQC experiment, revealed the presence of two sp^3 methines (one of which is oxygenated: δ_H 4.43, δ_C 80.1), five sp^3 methylenes, and five methyls (two of which are methoxy groups: δ_H 3.72, δ_C 52.2; δ_H 3.25, δ_C 48.8). In addition, the presence of three sp^2 methines (δ_H 5.44, δ_C 124.8; δ_H 6.03, δ_C 135.8; δ_H 5.47, δ_C 126.0) and of one quaternary sp^2 carbon (δ_C 133.3) indicated that two double bonds (one trisubstituted and one disubstituted) must be part of the molecule. The two remaining quaternary carbon atoms (δ_C 171.9 and 103.4) were attributable to an ester and to a ketal group, respectively.

The COSY spectrum of **2** disclosed the sequential arrangement of proton resonances indicating the presence of three spin systems (A−C, depicted in bold in Figure 1). The first one (A) encompasses a methyl-branched C_4 chain (from C-2 to C-5); the second spin system (B) builds up a C_5 unbranched chain starting from the disubstituted double bond, while the third spin system (C) includes only a sp^2 methine coupled to a methyl group. These moieties were connected through interpretation of the 2D HMBC spectrum (key $^{2,3}J_{CH}$ correlations are depicted in Figure 1). In particular, cross-peaks of 12-Me with C-11, C-12, and C-13 allowed us to join moieties B and C through C-12; analogously, the cross-peaks of H_2-5, H_2-7, and the methoxy group resonating at δ_H 3.25 with C-6 established this carbon as the connection point for moieties A and

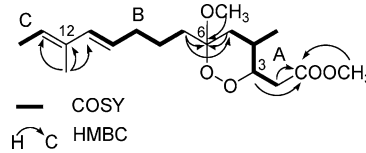

Figure 1. NMR COSY and key HMBC correlations detected for manadoperoxide A (**2**).

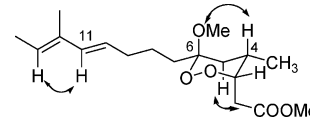

Figure 2. NMR ROESY correlations detected for manadoperoxide A (**2**).

B. Furthermore, the ester carbonyl (δ_C 171.9) was placed at C-1 on the basis of its HMBC correlations with H_2-2 and H-3. Finally, the presence of an endoperoxide bond connecting C-3 and C-6, accounting for the remaining unsaturation degree of the molecular formula, was supported by ^{13}C NMR resonances at δ_C 80.1 (C-3) and 103.4 (C-6), typical values for oxygenated carbons belonging to endoperoxyketal rings.[14]

The *E* geometry of the Δ^{10} double bond was deduced from the large vicinal coupling constant $J_{H\text{-}10/H\text{-}11}$ = 15.9 Hz. The spatial proximity (evidenced through a ROESY spectrum) between H-11 and H-13 indicated the *E* geometry of the Δ^{12} double bond. The ROESY spectrum (Figure 2) also allowed us to define the relative orientation of the three stereogenic carbons belonging to the six-membered ring. Particularly informative was the ROESY cross-peak of H-4 with OMe-6, indicating the *cis* diaxial orientation of these protons. On the other hand, the *trans* equatorial−axial orientation of H-3/H-4 was indicated by the small value of the vicinal coupling constant $J_{H\text{-}3/H\text{-}4}$ = 3.0 Hz and was supported by the ROESY cross-peak of H-5_{ax} with H-2a. This evidence allowed us to completely define the relative configuration of manadoperoxide A (**2**).

The determination of the absolute configuration at the three stereogenic centers of **2** was accomplished through application of the modified Mosher's method[15] on a semisynthetic derivative (Figure 3). The reductive cleavage (Zn/AcOH) of the endoperoxide bond yielded a product, whose quite complex ^{1}H and ^{13}C NMR spectra clearly indicated the presence of an equilibrium mixture including the hydroxyketone **6** and the two diastereomeric hemiketal

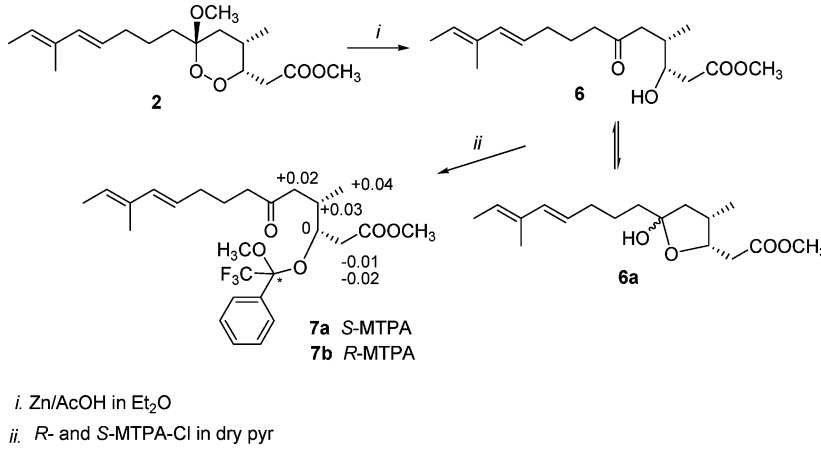

Figure 3. Application of the modified Mosher's method to a semisynthetic derivative of manadoperoxide A (**2**). $\Delta\delta(S - R)$ values are in ppm.

forms **6a**.[16] This mixture was allowed to react with *R*- and *S*-MTPA chloride to obtain the corresponding *S*- and *R*-MTPA esters (**7a** and **7b**), respectively. Analysis of the $\Delta\delta(S - R)$ values of the MTPA esters according to the Mosher's model indicated the *S* configuration at C-3. On the basis of the previously determined relative configuration, a 3*S*,4*S*,6*R* configuration was assigned to manadoperoxide A.

Three additional manadoperoxides (B−D, **3**−**5**) were isolated from the organic extract of *P.* cfr. *simplex*, and their stereostructural elucidation followed the same spectroscopic approach detailed above for **2**, including analysis of 1D and 2D NMR (COSY, HSQC, HMBC, ROESY) spectra. The complete assignment of proton and carbon resonances is reported in Tables 1 and 2, respectively (for **4** and **5**), or in the Experimental Section (for **3**). For brevity, only the significant differences between each of these molecules and manadoperoxide A will be highlighted in the following discussion. These differences are restricted to the length and/or functionalization of the "western" alkyl chain; accordingly, the H/C resonances from positions 1 to 8 of **3**−**5** were almost coincident to those of **2**. Furthermore, ROESY cross-peaks as well as proton coupling constants obtained for **3**−**5** confirmed that the relative configuration around the six-membered ring is also identical to that of compound **2**. Due to the limited amounts available for manadoperoxides B−D, and wanting to reserve some for biological tests, the absolute configurations at C-3/C-4/C-6 of **3**−**5** have not been determined; their stereostructures have been drawn extending the configurations deduced above for manadoperoxide A. In the case of manadoperoxide D (**5**), we decided to use an aliquot of the sample to determine the absolute configuration of the side chain stereocenters (see below).

Manadoperoxide B (**3**), $C_{19}H_{32}O_5$ by HRMS, contained only an additional methylene group compared to compound **2**. This group was easily located at C-14 (δ_H 2.09; δ_C 21.9) on the basis of the vicinal couplings of H_2-14 with both H-13 (δ_H 5.40, t) and the methyl H_3-15 (δ_H 1.00, t). Also in this case, the ROESY cross-peak H-11/H-13 indicated the *E* geometry of the Δ^{12}double bond.

Manadoperoxide C (**4**), $C_{16}H_{26}O_6$ by HRMS, showed a shortened side chain compared to compound **2**. Inspection of the ^1H and ^{13}C NMR (Tables 1 and 2, respectively) and COSY spectra of **4** indicated the presence of a single double bond, located at the terminus of the five-carbon spin system starting from H_2-7. The relatively low field resonances of H-10 (δ_H 6.78) and H-11 (δ_H 6.18) and the presence of a carbonyl resonance at δ_C 198.7, in the ^{13}C NMR spectrum of **4**, suggested the presence of a conjugated ketone group. This was supported by the $^{2,3}J$ HMBC cross-peaks of the relatively downfield shifted methyl singlet at δ_H 2.25 both with the ketone carbonyl (C-12) and with C-11. The coupling constant $J_{H\text{-}10,H\text{-}11} = 16.4$ Hz was indicative of the *E* geometry of Δ^{10}.

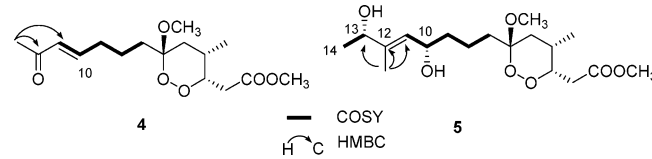

Figure 4. NMR COSY and key HMBC correlations detected for manadoperoxides C (**4**) (left) and D (**5**) (right).

The molecular formula of manadoperoxide D (**5**), $C_{18}H_{32}O_7$ by HRMS, indicated the presence of two additional oxygen atoms compared to compound **2**. The 1D NMR spectrum of **5**, analyzed with the help of COSY and HSQC spectra, disclosed the arrangement of the proton multiplets of the "western" side chain within two spin systems (Figure 4), comprising two oxygenated methines. The first spin system spans from H_2-7 to the single sp^2 methine H-11 (δ_H 5.45, δ_C 127.1) and includes an oxymethine at position 10 (δ_H 4.40, δ_C 70.1); the second spin system includes only the second oxymethine (δ_H 4.22, δ_C 72.8) coupled with a methyl group (δ_H 1.27, δ_C 17.9). The HMBC cross-peaks of 12-Me with C-11, C-12, and C-13 determined the connection for the above moieties, thus defining the gross structure of the "western" side chain for manadoperoxide D. The spatial proximity of 12-Me with H-10 (ROESY cross-peak) indicated the *E* geometry of the side chain double bond.

The absolute configuration at the two stereogenic carbons C-10 and C-13 of **5** was determined through application of the Riguera method for 1,*n*-diols.[17] To this aim, two aliquots of **5** were allowed to react with *R*- and *S*-MTPA chloride, obtaining the diesters **8a** and **8b**, respectively (see Supporting Information). Positive $\Delta\delta(S - R)$ values for protons going from H-9 to H-13 indicated, according to the Riguera model,[17] the 11*S*, 15*S* configuration.

The presence of methoxy groups in the structures **2**−**5** could raise the question whether these compounds are actually artifacts produced during the extraction process with MeOH. This possibility was ruled out through extraction of a small piece of the *P.* cfr. *simplex* with EtOH. Following the same chromatographic procedure described above, manadoperoxides were obtained.

Interestingly, Scheuer and co-workers isolated from a *Plakortis* sp. collected near Manado, in the same area of the sponge analyzed in this work, the C-6 epimer of manadoperoxide A, named manadic acid A methyl ester.[16] It should be noted that manadic acid or its esters were completely undetectable in the organic extract of *P.* cfr. *simplex*, and thus apparently the two *Plakortis* specimens elaborate the same secondary metabolite, but with the opposite configuration at a single carbon atom. A similar case, involving a different class of marine metabolites, has been recently reported by Crews and co-workers,[18] who discovered distinct *Theonella*

Table 3. *In Vitro* Antimalarial Activity of Manadoperoxides A−D (**2**−**5**) against D10 (CQ-S) and W2 (CQ-R) Strains of *P. falciparum*[a]

	D10 IC_{50}, μM	W2 IC_{50}, μM
1	0.87 ± 0.35	0.39 ± 0.13
2	6.88 ± 0.37	3.74 ± 0.92
3	6.76 ± 0.32	3.69 ± 0.88
4	4.54 ± 0.66	2.33 ± 0.48
5	10.38 ± 0.76	7.93 ± 0.68
chloroquine	0.026 ± 0.004	0.41 ± 0.06

[a] Data are means ± SD of three different experiments in triplicate.

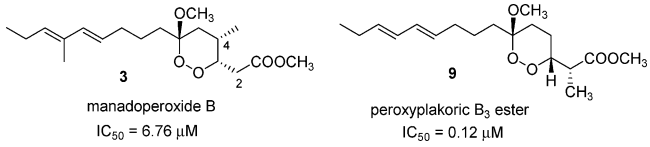

Figure 5. Comparison of chemical structure and activity of manadoperoxide A (**2**) with those of peroxyplakoric B_3 ester (**9**).

swinhoei populations producing either 2*S*-motuporin or 2*R*-motuporin. In our opinion, these intriguing observations are worthy of further investigations.

In this context, another interesting observation is related to the comparison between the chemical composition of the Indonesian *P.* cfr. *simplex* and that of a Caribbean specimen that we extensively investigated over the past few years.[7,19] We observed marked differences in the structures of the endoperoxide polyketides, which constitute the main secondary metabolites in both sponges. In particular, the Indonesian specimen elaborates compounds of the peroxyketal-type, while in the Caribbean one the methoxy group at C-6 is invariably replaced by a methyl/ethyl group. In the evaluation of this interesting observation, both a possible specific difference of Indonesian and Caribbean specimens and the biosynthetic role of microbial symbionts, demonstrated for the Caribbean *P. simplex*,[20] should be taken into account.

The endoperoxide derivatives **2**−**5** were assayed *in vitro* against D10 (chloroquine-sensitive, CQ-S) and W2 (chloroquine-resistant, CQ-R) strains of *P. falciparum* using the pLDH assay. The results (Table 3) evidenced moderate antimalarial activity (low μM range) against both CQ-R and CQ-S *P. falciparum* strains with no significant differences for the four manadoperoxides **2**−**5**. The variations in the side chains modestly influenced the antimalarial activity, with manadoperoxide C (**4**) slightly being the most active compound of the series. Furthermore, the IC_{50} values of **2**−**5** against the CQ-R strain were almost half of those (higher efficacy) against the CQ-S strain, as already found for plakortin analogues.[8−10]

The modest antimalarial activity of manadoperoxides could appear surprising upon comparison of the structures of the manadoperoxides (e.g., manadoperoxide B, **3**) with that of peroxyplakoric B_3 ester (**9**) (Figure 5), isolated in 1993 by Kobayashi et al. from a *Plakortis* sp.[14] In spite of the very small structural differences (a methyl group linked at C-2 in **9** in place of two methyl groups at C-4 and C-13 in **3**, in addition to a small variation in the side chain), compound **9** exhibited much higher *in vitro* antimalarial activity (IC_{50}: 0.12 μM on *P. falciparum* FCR3 cycloguanil-resistant strain from Gambia)[21] compared to **3**.

Table 4. Occurrence Rate (%) of 1,2-Dioxane Ring Conformations Considering PM6 Conformers within 5 kcal/mol from the Global Minimum

compound	chair A[a]	chair B[a]	boat A[a]	boat B[a]
2	0	85	15	0
3	5	72	23	0
4	3	81	13	3
5	7	80	10	3
1	82	6	11	1
9	37	37	26	0

[a] See Figure 8 for these conformations.

This unexpected difference can be rationalized on the basis of our recently published model for the antimalarial activity of 1,2-dioxanes.[11] We proposed that plakortin (**1**) and dihydroplakortin (**10**), upon reaction with Fe(II), generate a radical at O1, which is simultaneously transferred by means of a "through-space" mechanism to a "western" side chain carbon (Figure 6).[11] The resulting carbon radicals should represent the toxic species responsible for the antimalarial activity, similarly to artemisinin.[11] Because a concerted dissociative electron transfer (DET) mechanism was hypothesized for the plakortins, their structures must simultaneously orient all of the intramolecular reaction partners (i.e., Fe(II), O1, and the intramolecular radical shift partner) in order to trigger the production of the toxic carbon radical, thus implying two requirements for the bioactive conformation: (i) accessibility of endoperoxide oxygen atoms to Fe(II) and (ii) correct orientation of O1 with respect to reaction partners for an intramolecular (1,4 or 1,5) radical shift. Finally, the presence of additional Fe(II)-interacting atoms, other than the endoperoxide oxygens, could affect the antimalarial activity influencing the endoperoxide approach to Fe(II). This model is in agreement with the reported structure−activity relationships of plakortins, which evidenced the key role played by conformational parameters on the antimalarial activity of simple 1,2-endoperoxides.[10]

Based on the hypothesized mechanism of action, a molecular modeling study has been performed to account for the lower antimalarial activity of compounds **2**−**5** with respect to **1** and **9**. In order to sample the conformational space of **2**−**5** and **9**, an integrated computational analysis combining molecular dynamics and mechanics, as well as semiempirical (PM6) quantum mechanical calculations (see Experimental Section), was carried out. The generated conformers were grouped into families on the basis of their 1,2-dioxane ring conformation and ranked by their potential energy values (i.e., ΔE from the global energy minimum) (Table 4, Figure 7). The conformational search results were also analyzed by calculating occurrence rates and by measuring the distance between the endoperoxide oxygen O1 and possible partners on the "western" side chain for a "through-space" (1,4 or 1,5) intramo-

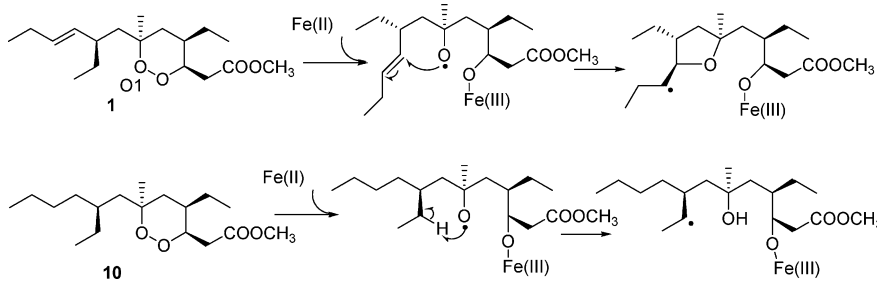

Figure 6. Mechanism proposed for the formation of the toxic side chain carbon radical for plakortin (**1**) (top) and dihydroplakortin (**10**) (bottom).

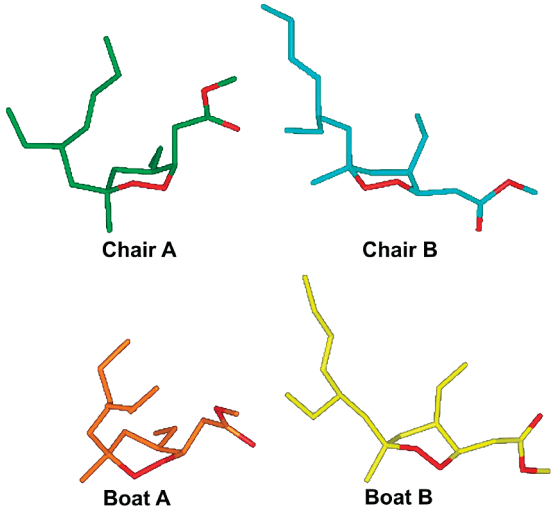

Figure 7. Lowest energy minima of each conformational family of the plakortin 1,2-dioxane ring. Carbons are in green (chair A), cyan (chair B), orange (boat A), and yellow (boat B); oxygens are in red. All hydrogens are omitted for clarity.

Table 5. PM6 Conformers of **3** Owning Interatomic Distances Suitable for a Radical Shift from O1 (≤ 3 Å) (Involved Atoms, Occurrence Percentages, 1,2-Dioxane Ring Conformations)

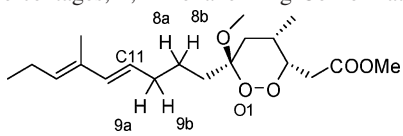

.

atom	chair A[a]	chair B[a]	boat A[a]	boat B[a]
C11	0%	2%	0%	0%
H9a	0%	9%	2%	0%
H9b	0%	3%	2%	0%
H8a	0%	25%	9%	0%
H8b	2%	18%	3%	0%

[a] Percentage of conformers within 5 kcal/mol from the global minimum having a distance between the involved atom and O1 of ≤3 Å.

lecular radical shift for all energetically accessible conformers, i.e., within 5 kcal/mol from the global minimum (Tables 5 and S1−S4).

The results were compared with those obtained by applying the same computational procedure to **1**.[10,11] In the case of this latter compound, chair A (Figure 7) represented the preferred conformation of the 1,2-dioxane ring (Table 4), due to the 1,3-diaxal steric effect between the ethyl group at C-4 and the alkyl side chain at C-6, as well as the bioactive one (Figure 8A). On the contrary, conformers with the same arrangement of the dioxane ring (chair A) (but with a different position of the substituents due to the inversion of configuration at C-3, C-4, and C-6) are scarcely present in the conformational space of compounds **2**−**5**, which showed a strong conformational preference for chair B (Table 4). This is likely due to the 1,3-diaxial steric effect between the methyl group at C-4 and the alkyl side chain at C-6, hampering chair A conformation for the **2**−**5** dioxane rings (Figure 8B). Furthermore, chair A conformers of **2**−**5** do not include significant amounts of side chain conformations bearing the intramolecular distances suitable for the possible "through-space" (1,4 or 1,5) intramolecular radical shift (Tables 5 and S2−S4). Indeed, as depicted in Figure 8B, the methyl group at C-4 hinders the approach of the "western" side chain to O1. As for chair B, which represents the most populated family of conformers for **2**−**5** (Table 4), a significant number of conformations bearing the required distances for hypothesized intramolecular shift are included (Table 5). However, when chair B conformers were analyzed, Connolly surfaces revealed that accessibility to the

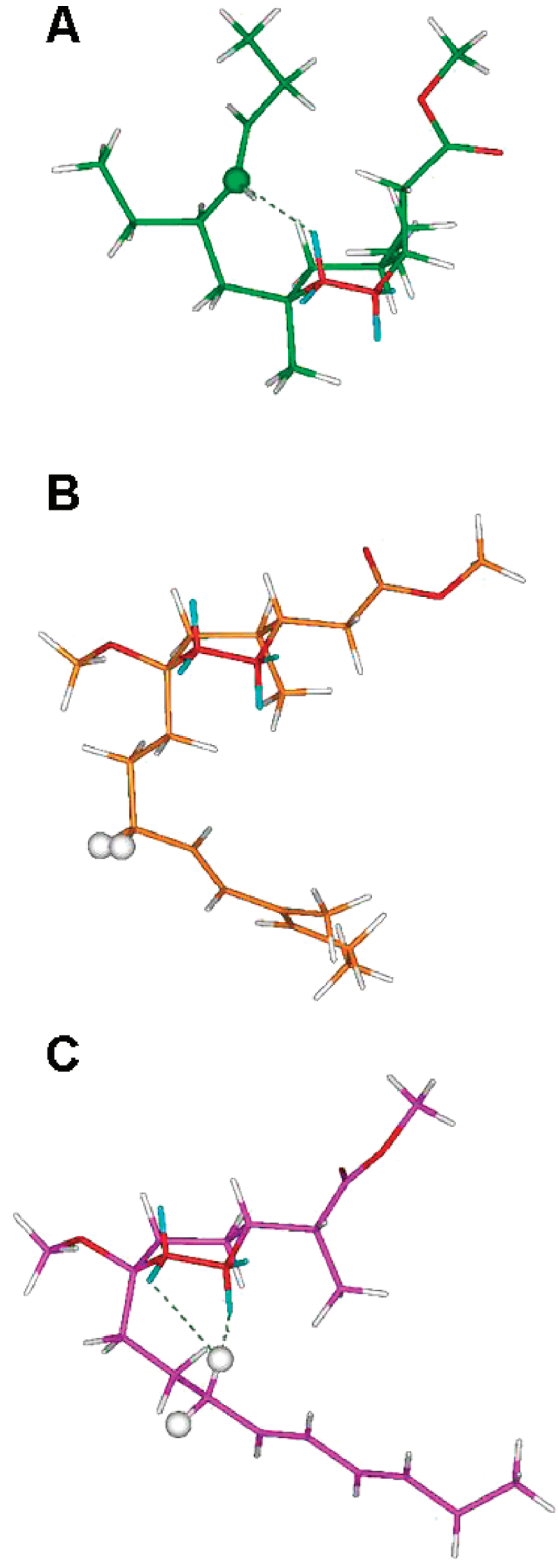

Figure 8. Comparison between chair A bioactive conformations of plakortin (**1**) (A, green), compound **9** (C, magenta), and the corresponding conformer of manadoperoxide A (**2**) (B, orange). The molecules are colored by atom type (O = red, H = white, and lone pairs = cyan). Possible partners in a "through-space" intramolecular radical shift are shown as balls.

endoperoxide oxygen lone pairs is impaired by the axial position of the methoxy substituent at C-6 (Figure S2). In summary, for compounds **2**−**5** (i) the endoperoxide linkage is unlikely to be accessible to the heme iron in the most populated chair B

conformers, while (ii) in the minimally populated chair A conformers, the O1 radical cannot evolve to produce a toxic C-centered radical.

Compound **9**, lacking the methyl substituent at C-4, presents 37% of low-energy conformers adopting chair A as the 1,2-dioxane ring conformation (Table 4), and one-third of them have distances suitable for a "through-space" (1,4 or 1,5) intramolecular radical shift from O1 to possible partners on the "western" side chain (Figure 8C and Table S1, Supporting Information). As in the case of **2**−**5** and contrarily to what happened for **1**, compound **9** presents an axially oriented alkyl chain at C-6 when the 1,2-dioxane ring assumes the chair A conformation. As a consequence, as illustrated in Figure 8C, in the putative bioactive conformation of **9** the methoxy group at C-6 is positioned in equatorial position, thus favoring the endoperoxide approach to the Fe(II)-heme. Finally, according to the hypothesized mechanism of antimalarial action, the formation of a carbon radical on the "western" side chain of **9** is more favored with respect to the formation of a carbon radical on the "western" side chain of **1**. Taken together, these results can account for the comparable antimalarial activity shown by **1** and **9** against *P. falciparum* drug-resistant strains.

Conclusions

Throughout this paper we have reported the isolation and the stereostructure elucidation of four new endoperoxide peroxyketal derivatives (**2**−**5**) from the Indonesian sponge *P.* cfr. *simplex*. Their *in vitro* antimalarial activity is quite modest compared to that of the previously reported plakortin (**1**) and peroxyplakoric methyl ester B_3 (**9**). In light of our recently published hypothesis for the mechanism of action of simple 1,2-dioxanes, the computational analysis herein reported provides a reasonable explanation for this marked difference in the antimalarial activity. Our explanation reveals that minor structural changes can have a deep impact on the antimalarial activity when they affect the conformational behavior of the molecule and, consequently, affect the molecule's ability to interact with heme and produce the toxic C-centered radical, which is responsible for the final activity.

Experimental Section

General Experimental Procedures. Optical rotations ($CHCl_3$) were measured at 589 nm on a Perkin-Elmer 192 polarimeter. IR (KBr) spectra were recorded on a Bruker model IFS-48 spectrophotometer. UV spectra were obtained in CH_3CN using a Beckman DU70 spectrophotometer. ^1H (500 MHz) and ^{13}C (125 MHz) NMR spectra were measured on a Varian INOVA spectrometer. Chemical shifts were referenced to the residual solvent signal ($CDCl_3$: δ_H 7.26, δ_C 77.0). Homonuclear ^1H connectivities were determined by the COSY experiment; one-bond heteronuclear $^1H-^{13}C$ connectivities by the HSQC experiment; two- and three-bond $^1H-^{13}C$ connectivities by gradient-HMBC experiments optimized for a $^{2,3}J$ of 8 Hz. Through-space ^1H connectivities were evidenced by using a ROESY experiment with a mixing time of 500 ms. ESIMS spectra were performed on a LCQ Finnigan MAT mass spectrometer. Medium-pressure liquid chromatography was performed on a Büchi apparatus using a silica gel (230−400 mesh) column; HPLC were achieved on a Knauer apparatus equipped with a refractive index detector. The Knauer HPLC apparatus was used to purify and assess purity (>95%) of all final products. LUNA (normal phase, SI60, 250 × 4 mm) (Phenomenex) columns were used, with elution with EtOAc/*n*-hexane mixtures and 0.7 mL/min as the flow rate.

Animal Material. A specimen of *Plakortis* cfr. *simplex* (order Homosclerophorida, family Plakinidae) was collected in January 2008 along the coasts of the Bunaken island in the Bunaken Marine Park of Manado. Differences in spicule size between the Indonesian and Caribbean specimens suggest caution in this specific attribution. A voucher sample (no. MAN08-02) has been deposited at the Dipartimento di Chimica delle Sostanze Naturali, Università di Napoli Federico II.

Extraction and Isolation. After homogenization, the organism was exhaustively extracted, in sequence, with MeOH and $CHCl_3$ (dry weight after extraction 199.3 g). The combined extracts (8.6 g) were subjected to chromatography over a silica column (230−400 mesh) eluting with a solvent gradient of increasing polarity from hexane to MeOH. Fractions that eluted with *n*-hexane/EtOAc, 9:1, were subjected to repeated column and HPLC chromatographies (*n*-hexane/EtOAc, 95:5), affording manadoperoxides A (**2**, 8.5 mg) and B (**3**, 6.2 mg) in the pure state. Fractions that eluted with *n*-hexane/EtOAc, 8:2, were rechromatographed by HPLC (*n*-hexane/EtOAc, 85:15) to give manadoperoxide C (**4**, 2.0 mg). Fractions that eluted with *n*-hexane/EtOAc, 3:7, were rechromatographed by HPLC (*n*-hexane/EtOAc, 4:6), affording pure manadoperoxide D (**5**, 3.1 mg).

Manadoperoxide A (2): colorless, amorphous solid; $[\alpha]^{25}_D$ −5.2 (*c* 0.3, $CHCl_3$); UV (CH_3CN) λ_{max} (log ε) 233 (4.3) nm; IR (KBr) ν_{max} 2970, 1730, 1455, 1287 cm^{-1}; ^1H NMR ($CDCl_3$, 500 MHz) Table 1; ^{13}C NMR ($CDCl_3$, 125 MHz) Table 2; (+)-ESIMS *m/z* 327 $[M + H]^+$, 349 $[M + Na]^+$; HRESIMS *m/z* 327.2177 (calcd for $C_{18}H_{31}O_5$ 327.2171).

Manadoperoxide B (3): colorless, amorphous solid; $[\alpha]^{25}_D$ −5.5 (*c* 0.2 in $CHCl_3$); UV (CH_3CN) λ_{max} (log ε) 233 (4.3) nm; IR (KBr) ν_{max} 2970, 1730, 1455, 1287 cm^{-1}; ^1H NMR ($CDCl_3$, 500 MHz) δ_H 6.03 (1H, d, J = 15.9 Hz, H-11), 5.47 (1H, dt, J = 15.9, 6.0 Hz, H-10), 5.40 (1H, t, J = 6.1 Hz, H-13), 4.43 (1H, m, H-3), 3.72 (3H, s, 1-OMe), 3.26 (3H, s, 6-OMe), 2.97 (1H, dd, J = 15.5, 9.5 Hz, H-2a), 2.57 (1H, m, H-4), 2.44 (1H, dd, J = 15.5, 4.5 Hz, H-2b), 2.09 (2H, overlapped, H-14), 2.07 (2H, overlapped, H-9), 1.70 (3H, s, 12-Me), 1.69 (1H, overlapped, H-5a), 1.66 (1H, overlapped, H-7a), 1.40 (2H, overlapped, H-8), 1.36 (1H, overlapped, H-7b), 1.28 (1H, m, H-5b), 1.00 (3H, t, J = 7.1 Hz, H-15), 0.84 (3H, d, J = 7.1 Hz, 4-Me); ^{13}C NMR ($CDCl_3$, 125 MHz) δ_C 172.5 (C, C-1), 136.0 (CH, C-11), 133.8 (CH, C-13), 133.3 (C, C-13), 125.8 (CH, C-10), 103.4 (C, C-6), 80.2 (CH, C-3), 52.2 (CH_3, 1-OMe), 48.8 (CH_3, 6-OMe), 34.6 (CH_2, C-5), 33.6 (CH_2, C-9), 32.1 (CH_2, C-7), 31.4 (CH_2, C-2), 27.6 (CH, C-4), 23.5 (CH_2, C-8), 21.9 (CH_2, C-14), 17.0 (CH_3, C-4-Me), 15.0 (CH_3, C-12-Me), 13.0 (CH_3, C-15); (+)-ESIMS *m/z* 341 $[M + H]^+$, 363 $[M + Na]^+$; HRESIMS *m/z* 341.2333 (calcd for $C_{19}H_{33}O_5$ 341.2328).

Manadoperoxide C (4): colorless, amorphous solid; $[\alpha]^{25}_D$ −3.3 (*c* 0.1, $CHCl_3$); UV (CH_3CN) λ_{max} (log ε) 236 (4.0) nm; IR (KBr) ν_{max} 2956, 1720, 1680, 1435, 1295 cm^{-1}; ^1H NMR ($CDCl_3$, 500 MHz) Table 1; ^{13}C NMR ($CDCl_3$, 125 MHz) Table 2; (+)-ESIMS *m/z* 315 $[M + H]^+$, 337 $[M + Na]^+$; HRESIMS *m/z* 315.1801 (calcd for $C_{16}H_{27}O_6$, 315.1808).

Manadoperoxide D (5): colorless, amorphous solid; $[\alpha]^{25}_D$ −4.2 (*c* 0.2, $CHCl_3$); UV (CH_3CN) λ_{max} (log ε) 235 (4.5) nm; IR (KBr) ν_{max} 3200, 1735, 1450, 1250 cm^{-1}; ^1H NMR ($CDCl_3$, 500 MHz) Table 1; ^{13}C NMR ($CDCl_3$, 125 MHz) Table 2; (+)-ESIMS *m/z* 361 $[M + H]^+$, 383 $[M + Na]^+$; HRESIMS *m/z* 361.2222 (calcd for $C_{18}H_{33}O_7$, 361.2226).

Reductive Cleavage of Manadoperoxide A (2) and Reaction with *R*- and *S*-MTPA Chloride. Compound **2** (5.0 mg, 15.3 μmol) in 100 μL of dry ether was treated with 50 μL of acetic acid and an excess (20 mg) of Zn dust and then stirred vigorously for 24 h at room temperature (rt). After confirmation of disappearance of the starting material by TLC, the solution was neutralized with Na_2CO_3 and the solid removed by filtration. The solvent was then evaporated, and the obtained product was partitioned between H_2O and $CHCl_3$. An aliquot of the organic phase (1.0 mg) was treated with *R*-MTPA chloride (30 μL) in 400 μL of dry pyridine with a catalytic amount of DMAP overnight at rt. Then, the solvent was removed and the product was purified by HPLC (*n*-hexane/EtOAc, 97:3) to obtain the *S*-MTPA ester **7a** (1.3 mg, 80% yield). When the organic phase (1.0 mg) was treated with *S*-MTPA chloride, following the same procedure, 1.3 mg (80% yield) of *R*-MTPA ester **7b** was obtained.

***S*-MTPA ester (7a):** amorphous solid; ESIMS (positive ions) *m/z* 485 $[M + H]^+$; ^1H NMR ($CDCl_3$) δ 7.35 and 7.45 (MTPA phenyl protons), 6.03 (1H, d, J = 15.9 Hz, H-11), 5.65 (H-3, m); 5.45 (1H, q, J = 6.9 Hz, H-13), 5.42 (1H, dt, J = 15.9, 6.0 Hz, H-10), 3.72 (3H, s, 1-OMe), 3.55 (3H, s, 6-OMe), 2.77 (1H, dd, J = 15.5, 9.5 Hz, H-2a), 2.54 (1H, m, H-4), 2.44 (1H, dd, J = 15.5, 4.5 Hz, H-2b), 2.42 (1H, m, H-5a), 2.41 (2H, t, J = 7.4 Hz, H-7), 2.17 (1H, m, H-5b), 2.09 (2H, m, H-9), 1.70 (3H, overlapped, H-14), 1.68 (3H, s, 12-Me), 1.68 (2H, overlapped, H-8), 0.89 (3H, d, J = 7.1 Hz, 4-Me).

***R*-MTPA ester (7b):** amorphous solid; ESIMS (positive ions) *m/z* 485 $[M + H]^+$; ^1H NMR ($CDCl_3$) δ 7.32 and 7.55 (MTPA phenyl protons), 6.03 (1H, d, J = 15.9 Hz, H-11), 5.65 (H-3, m); 5.45 (1H, q,

J = 6.9 Hz, H-13), 5.42 (1H, dt, J = 15.9, 6.0 Hz, H-10), 3.72 (3H, s, 1-OMe), 3.55 (3H, s, 6-OMe), 2.78 (1H, dd, J = 15.5, 9.5 Hz, H-2a), 2.51 (1H, m, H-4), 2.46 (1H, dd, J = 15.5, 4.5 Hz, H-2b), 2.40 (1H, m, H-5a), 2.41 (2H, t, J = 7.4 Hz, H-7), 2.15 (1H, m, H-5b), 2.08 (2H, m, H-9), 1.70 (3H, overlapped, H-14), 1.68 (3H, s, 12-Me), 1.67 (2H, overlapped, H-8), 0.85 (3H, d, J = 7.1 Hz, 4-Me).

Reaction of 5 with *R*- and *S*-MTPA Chloride. Compound **5** (1.0 mg, 2.8 μmol) was treated with *R*-MTPA chloride (30 μL) in 400 μL of dry pyridine with a catalytic amount of DMAP overnight at rt. Then, the solvent was removed and the product was purified by HPLC (*n*-hexane/EtOAc, 97:3) to obtain the *S*-MTPA diester **8a** (1.8 mg, 81% yield). When compound **5** (1.0 mg, 2.8 μmol) was treated with *S*-MTPA chloride, following the same procedure, 1.7 mg (76% yield) of *R*-MTPA ester **8b** was obtained.

***S*-MTPA ester (8a):** amorphous solid; ESIMS (positive ions) *m*/*z* 793 $[M + H]^+$; ^{1}H NMR ($CDCl_3$) δ 7.35 and 7.45 (MTPA phenyl protons), 5.61 (1H, m, H-10), 5.45 (1H, d, J = 8.7 Hz, H-11), 5.41 (1H, q, J = 7.1 Hz, H-13), 4.37 (1H, m, H-3), 3.70 (3H, s, 1-OMe), 3.55 (6H, s, MTPA-OMe), 3.17 (3H, s, 6-OMe), 2.83 (1H, dd, J = 15.5, 9.5 Hz, H-2a), 2.47 (1H, m, H-4), 2.37 (1H, dd, J = 15.5, 4.5 Hz, H-2b), 1.77 (3H, s, 12-Me), 1.65 (1H, overlapped, H-5a), 1.60 (1H, m, H-9a), 1.55 (2H, m, H-7), 1.40 (1H, m, H-9b), 1.35 (2H, overlapped, H-8), 1.35 (1H, overlapped, H-5b), 1.31 (3H, d, J = 7.1 Hz, H-14), 0.78 (3H, d, J = 7.1 Hz, 4-Me).

***R*-MTPA ester (8b):** amorphous solid; ESIMS (positive ions) *m*/*z* 793 $[M + H]^+$; ^{1}H NMR ($CDCl_3$) δ 7.32 and 7.55 (MTPA phenyl protons), 5.59 (1H, m, H-10), 5.43 (1H, d, J = 8.7 Hz, H-11), 5.38 (1H, q, J = 7.1 Hz, H-13), 4.37 (1H, m, H-3), 3.70 (3H, s, 1-OMe), 3.55 (6H, s, MTPA-OMe), 3.22 (3H, s, 6-OMe), 2.83 (1H, dd, J = 15.5, 9.5 Hz, H-2a), 2.45 (1H, m, H-4), 2.37 (1H, dd, J = 15.5, 4.5 Hz, H-2b), 1.75 (3H, s, 12-Me), 1.65 (1H, overlapped, H-5a), 1.60 (1H, m, H-9a), 1.55 (2H, m, H-7), 1.37 (1H, m, H-9b), 1.37 (1H, overlapped, H-5b), 1.34 (2H, overlapped, H-8), 1.29 (3H, d, J = 7.1 Hz, H-14), 0.78 (3H, d, J = 7.1 Hz, 4-Me).

Molecular Modeling. Molecular modeling calculations were performed on a SGI Origin 200 8XR12000 workstation, while molecular modeling graphics were visualized on a SGI Octane 2 workstation. Compounds **2**−**5** and **9** were built using the Insight 2005 Builder module (Accelrys Software Inc.). Atomic potentials and charges were assigned using the CFF91 force field.[22]

The conformational space of the compounds was sampled through 200 cycles of simulated annealing ($\varepsilon = 80r$) applying the following protocol: the system was heated to 1000 K over 2000 fs (time step = 3.0 fs); the temperature of 1000 K was applied to the system for 2000 fs (time step = 3.0 fs) with the aim of surmounting torsional barriers; successively, temperature was linearly reduced to 300 K in 1000 fs (time step = 1.0 fs). The resulting structures were subjected to energy minimization within the Insight 2005 Discover module (CFF91 force field; $\varepsilon = 80r$) until the maximum rms derivative was less than 0.001 kcal/Å, using conjugate gradient[23] as the minimization algorithm. All conformers obtained from molecular dynamics and mechanics calculations were subjected to a full geometry optimization by semiempirical calculations, using the quantum mechanical method PM6[24] in the Mopac2007 package[25] and EF[26] (eigenvector following routine) as the geometry optimization algorithm. The GNORM value was set to 0.01. To reach a full geometry optimization, the criterion for terminating all optimizations was increased by a factor of 100, using the keyword PRECISE. Resulting conformers were grouped into families on the basis of their 1,2-dioxane ring conformation and ranked by their potential energy values (i.e., ΔE from the global energy minimum). Occurrence rates, together with the distance between O1 and possible partners for a "through-space" (1,4 and 1,5) intramolecular radical shift, were calculated for all conformers. The accessible surface area of the endoperoxide oxygens' lone pairs has been evaluated by calculating Connolly surfaces (Insight 2005, Accelrys Software Inc.).

***In Vitro* Drug Susceptibility Assay of *P. falciparum*.** The CQ-sensitive (D10) and the CQ-resistant (W2) strains of *P. falciparum* were cultured *in vitro* as described by Trager and Jensen.[27] Parasites were maintained in human type A-positive red blood cells at 5% hematocrit in RPMI 1640 (Gibco BRL, $NaHCO_3$ 24 mM) medium with the addition of 1% AlbuMaxII (Invitrogen), 0.01% hypoxantine, 20 mM Hepes, and 2 mM glutamine. The cultures were maintained at 37 °C in a standard gas mixture consisting of 1% O_2, 5% CO_2, and 94% N_2. Test compounds were dissolved in either H_2O or DMSO and then diluted with medium to achieve the required concentrations (final DMSO concentration <1%, which is nontoxic to the parasite). Compounds were added in serial dilutions to 96-well flat-bottom microplates (COSTAR). Asexual parasite stages derived from asynchronous cultures with parasitemia of 1−1.5% were aliquoted into the plates (final hematocrit 1%) and incubated for 72 h at 37 °C. Parasite growth was determined spectrophotometrically (OD_{650}) by measuring the activity of the parasite lactate dehydrogenase (LDH), according to a modified version of Makler's method in control and treated cultures.[28] Chloroquine was used as reference control. The antiplasmodial activity is expressed as the 50% inhibitory concentration (IC_{50}). Each IC_{50} value presented in Table 3 is the mean and standard deviation of three separate experiments performed in triplicate.

Acknowledgment. This work was supported by the FP6-EU Project 18834-AntiMal and by MIUR (PRIN2008: Leads ad Attività Antimalarica di Origine Naturale: Isolamento, Ottimizzazione e Valutazione Biologica) and was partially conducted during the Master Course "Tropical Marine Biodiversity and Natural Products" of Università Politecnica delle Marche. Mass and NMR spectra were recorded at the "Centro di Ricerca Interdipartimentale di Analisi Strumentale" of the University of Naples "Federico II". The assistance of the staff is gratefully acknowledged. M.P., Italian Malaria Network, was funded by Compagnia di San Paolo, Torino, Italy.

Supporting Information Available: Copies of NMR spectra for **2**−**5** and material from computational calculations. This material is available free of charge via the Internet at http://pubs.acs.org.

References and Notes

(1) Data taken from Malaria Foundation International, http://www.malaria.org and linked sites.
(2) Klayman, D. L. *Science* **1985**, *228*, 1049–1055, and references therein.
(3) Longo, M.; Zanoncelli, S.; Manera, D.; Brughera, M.; Colombo, P.; Lansen, J.; Mazue, G.; Gomes, M.; Taylor, W. J.; Olliaro, P. *Reprod. Toxicol.* **2006**, *21*, 83–93.
(4) Jefford, C. W. *Drug Discovery Today* **2007**, *12*, 487–495.
(5) Dondorp, A. M.; Nosten, F.; Yi, P.; Das, D.; Phyo, A. P.; Tarning, J.; Lwin, K. M.; Ariey, F.; Hanpithakpong, W.; Lee, S. J.; Ringwald, P.; Silamut, K.; Imwong, M.; Chotivanich, K.; Lim, P.; Herdman, T.; An, S. S.; Yeung, S.; Singhasivanon, P.; Day, N. P.; Lindegardh, N.; Socheat, D.; White, N. J. *N. Engl. J. Med* **2009**, *361*, 455–467.
(6) Fattorusso, E.; Taglialatela-Scafati, O. *Mar. Drugs* **2009**, *7*, 130–152.
(7) Cafieri, F.; Fattorusso, E.; Taglialatela-Scafati, O.; Ianaro, A. *Tetrahedron* **1999**, *55*, 7045–7056.
(8) Fattorusso, E.; Parapini, S.; Campagnuolo, C.; Basilico, N.; Taglialatela-Scafati, O.; Taramelli, D. *J. Antimicrob. Chemother.* **2002**, *50*, 883–888.
(9) Campagnuolo, C.; Fattorusso, E.; Romano, A.; Taglialatela-Scafati, O.; Basilico, N.; Parapini, S.; Taramelli, D. *Eur. J. Org. Chem.* **2005**, 5077–5083.
(10) Fattorusso, C.; Campiani, G.; Catalanotti, B.; Persico, M.; Basilico, N.; Parapini, S.; Taramelli, D.; Campagnuolo, C.; Fattorusso, E.; Romano, A.; Taglialatela-Scafati, O. *J. Med. Chem.* **2006**, *49*, 7088–7094.
(11) Taglialatela-Scafati, O.; Fattorusso, E.; Romano, A.; Scala, F.; Barone, V.; Cimino, P.; Stendardo, E.; Catalanotti, B.; Persico, M.; Fattorusso, C. *Org. Biomol. Chem.* **2010**, *8*, 846–856.
(12) Fattorusso, E.; Romano, A.; Taglialatela-Scafati, O.; Achmad, M. J.; Bavestrello, G.; Cerrano, C. *Tetrahedron Lett.* **2008**, *49*, 2189–2192.
(13) Fattorusso, E.; Romano, A.; Taglialatela-Scafati, O.; Irace, C.; Maffettone, C.; Bavestrello, G.; Cerrano, C. *Tetrahedron* **2009**, *65*, 2898–2904.
(14) Kobayashi, M.; Kondo, K.; Kitagawa, I. *Chem. Pharm. Bull.* **1993**, *41*, 1324–1326.
(15) Ohtani, I.; Kusumi, T.; Kashman, Y.; Kakisawa, H. *J. Am. Chem. Soc.* **1991**, *113*, 4092–4096.
(16) Ichiba, T.; Scheuer, P. J.; Kelly-Borges, M. *Tetrahedron* **1995**, *51*, 12195–12202. See also corrigenda in *Tetrahedron* **1996**, *52*, 14079.
(17) Freire, F.; Seco, J. M.; Quinoa, E.; Riguera, R. *J. Org. Chem.* **2005**, *70*, 3778–3790.
(18) Wegerski, C. J.; Hammond, J.; Tenney, K.; Matainaho, T.; Crews, P. *J. Nat. Prod.* **2007**, *70*, 89–94.
(19) Costantino, V.; Fattorusso, E.; Menna, M.; Taglialatela-Scafati, O. *Curr. Med. Chem.* **2004**, *11*, 1671–1692.
(20) Laroche, M.; Imperatore, C.; Grozdanov, L.; Costantino, V.; Mangoni, A.; Hentschel, U.; Fattorusso, E. *Mar. Biol.* **2007**, *151*, 1365–1373.
(21) Murakami, N.; Kawanishi, M.; Itagaki, S.; Horii, T.; Kobayashi, M. *Tetrahedron Lett.* **2001**, *42*, 7281–7285.

(22) Maple, J. R.; Hwang, M. J.; Stockfisch, T. P.; Dinur, U.; Waldman, M.; Ewig, C. S.; Hagler, A. T. *J. Comput. Chem.* **1994**, *15*, 162–182.
(23) Fletcher, R. Unconstrained Optimization. In *Pratical Methods of Optimization*; John Wiley & Sons: New York, 1980; Vol. 1.
(24) Stewart, J. J.P. *MOPAC2007*; Stewart Computational Chemistry: Colorado Springs, CO, 2007, HTTP://OpenMOPAC.net.
(25) Stewart, *J. Mol. Model.* **2007**, *13*, 1173–1213.
(26) Baker, J. *J. Comput. Chem.* **1986**, *7*, 385–395.
(27) Trager, W.; Jensen, J. B. *Science* **1976**, *193*, 673–675.
(28) Makler, M.; Hinrichs, D. *Am. J. Trop. Med. Hyg.* **1993**, *48*, 205–210.

NP100196B